

Observation of Optical Spin Symmetry Breaking in Nanoapertures

Yuri Gorodetski, Nir Shitrit, Itay Bretner, Vladimir Kleiner, and Erez Hasman*

Micro and Nanooptics Laboratory, Faculty of Mechanical Engineering, and Russell Berrie Nanotechnology Institute, Technion—Israel Institute of Technology, Haifa 32000, Israel

Received May 6, 2009; Revised Manuscript Received June 11, 2009

ABSTRACT

Observation of a spin symmetry breaking effect in plasmonic nanoscale structures due to spin–orbit interaction is presented. We demonstrate a nanoplasmonic structure which exhibits a crucial role of an angular momentum (AM) selection rule in a light-surface plasmon scattering process. In our experiment, the intrinsic AM (spin) of the incident radiation is coupled to the extrinsic momentum (orbital AM) of the surface plasmons via spin–orbit interaction. Due to this effect, we achieved a spin-controlled enhanced transmission through a coaxial nanoaperture.

A wide spectrum of plasmonic nanostructures has been studied recently due to their physical and technological impact.^{1–4} Plasmonic systems have been shown to be resonantly excited when the linear momentum selection rule is fulfilled.^{4–8} However, conservation of total angular momentum in a closed physical system results in additional selection rules related to angular momentum (AM).^{9–11} The AM of an optical beam comprises the intrinsic component, the spin, associated with the handedness of the circular polarization, and the extrinsic component, orbital AM (OAM), associated with a spiral phase front.^{12–15} Here, we demonstrate a plasmonic nanostructure which exhibits a crucial role of an AM selection rule in a light-surface plasmon scattering process. In our experiment, the intrinsic AM of the incident radiation is coupled to the extrinsic momentum of the surface plasmons via *spin–orbit interaction*, which is manifested by a geometric Berry phase.¹⁶ Due to this effect, we achieved a symmetry breaking resulting in a spin-dependent enhanced transmission through coaxial nanoapertures even in rotationally symmetric structures. The analogy with systems that exhibit a set of allowed transitions defined by AM selection rules provides a convenient tool for understanding the behavior of complex plasmonic nanostructures. We believe that spin-based plasmonic effects provide additional physical insight into the phenomenon of extraordinary light transmission^{4,6} and inspire one for a new type of *spinoptics* nanodevices.

The dynamics of various physical systems, including optical systems, are substantially characterized by their AM. In an optical paraxial beam with a spiral phase distribution ($\phi = -l\varphi$, where φ is the azimuthal angle in polar coordinates, and the integer number l is the

topological charge), the total AM per photon, in units of \hbar (normalized AM), was shown to be $j = (\sigma + l)$, where $\sigma = 1$ stands for the spin state $|\sigma_+\rangle$ (right-handed circular polarization) and $\sigma = -1$ stands for the spin state $|\sigma_-\rangle$ (left-handed circular polarization).¹⁷ In accordance with fundamental physical principles, resonant excitation of an electromagnetic eigenmode requires that the exciting wave match the excited mode both with its linear and with its angular momentum. This required matching imposes certain restrictions on the excitation process, selection rules. Here, we investigate the spin-dependent behavior of a nanoscale plasmonic system resulting from the AM selection rule. In our experiment, we excited coaxial nanoapertures in a thin metal film. The element consisted of a matrix of 6×14 coaxial apertures milled by a focused ion beam (FIB; FEI Strata 400s dual beam system, Ga⁺, 30 keV, 46 pA) into a 200 nm thick gold film evaporated onto a glass wafer. The inner and the outer radii of the ring slit were 250 and 350 nanometers, respectively.

For the first experiment all apertures were surrounded by a shallow (70 nm deep) spiral periodic corrugation (see Figure 1b) with a period of 500 nm and a pitch of 2 periods. The handedness of the spirals corresponding to the word “SPiN” was opposite to all the other spirals. The matrix was illuminated by a collimated white beam from a xenon arc lamp (Oriel 6263) whose circular polarization (spin) was altered by a quarterwave plate (liquid crystal Meadowlark H7160). A picture of the transmitted light for the spin states $|\sigma_+\rangle$ and $|\sigma_-\rangle$, and for the linear polarization ($|\sigma_+\rangle + |\sigma_-\rangle$), was captured by a camera and is presented in Figure 1a. The experimental results show that when the incident spin is opposite to the handedness of the spiral grating, the intensity of the transmitted light is enhanced. Accordingly,

* Corresponding author, mehasman@tx.technion.ac.il.

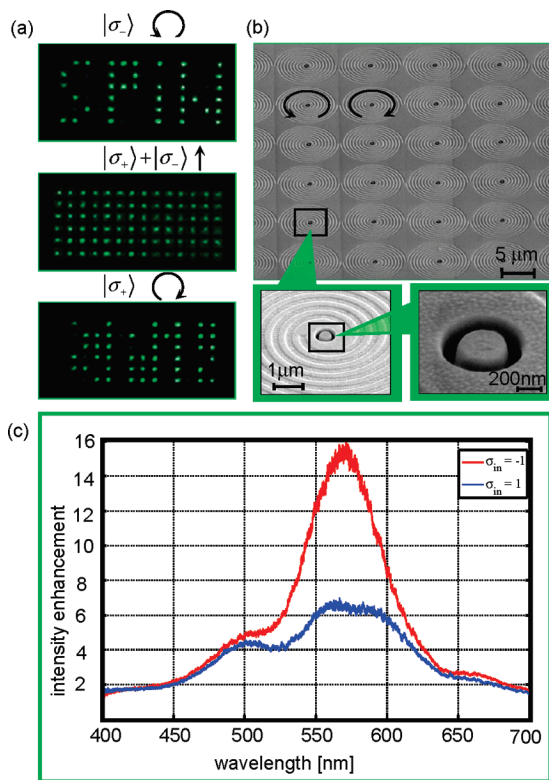


Figure 1. Spin-dependent transmission through coaxial nanoapertures. (a) Light transmission measured from the element for $|\sigma_{-}\rangle$, $|\sigma_{+}\rangle + |\sigma_{-}\rangle$ and $|\sigma_{+}\rangle$ illuminations. (b) Scanning electron microscopy (SEM) picture of the element used in the experiment. Spiral corrugations were either left-handed or right-handed, depicted with a counterclockwise or clockwise arrow, respectively. The magnified SEM pictures of a single element and a coaxial nanoaperture are also presented. (c) Spectral transmission enhancement for $|\sigma_{-}\rangle$ (red line) and $|\sigma_{+}\rangle$ (blue line). The spectrum was normalized by the transmission measured for coaxial apertures without corrugations.

the word “SPiN” written with right-handed spirals is lit up when illuminated by $|\sigma_{-}\rangle$ light. For $|\sigma_{+}\rangle$ illumination, the contrast is reversed. Linearly polarized illumination results in the same transmission for all nanoapertures: as a result, the letters are indistinguishable from the background.

A spectral transmission through a similarly structured array of only right-handed spirals was measured by a spectrometer (Horriba Jobin Yvon, iHR320) and normalized by transmission through a coaxial aperture array without corrugations. In Figure 1c a resonant peak corresponding to a Q -factor of 9 is clearly observed for $|\sigma_{-}\rangle$ illumination around 570 nm. The light transmission at the peak was found to be enhanced by a factor of 16 relative to an uncorrugated aperture array. The spectral transmission of a $|\sigma_{+}\rangle$ illumination does not exhibit any substantial resonance. Observation of a considerable spin-dependent transmission (with a ratio of about 3) is presented.

The excitation of electromagnetic eigenmodes inside a nanoaperture by surface waves is constrained by the AM selection rule, which is given by

$$l_{SM} = l_{GM} \quad (1)$$

where l_{SM} is the normalized OAM of the surface mode and

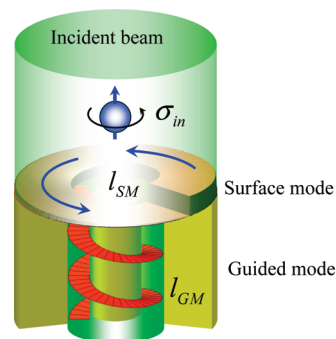


Figure 2. The mechanism of the nanoaperture’s excitation controlled by the AM selection rules. The incident beam bears the intrinsic angular momentum of σ_{in} . The excited surface mode acquires the orbital angular momentum of l_{SM} as a result of the spin–orbit interaction. The guided mode with l_{GM} is excited only if the selection rule is satisfied.

l_{GM} is the normalized OAM of the guided mode inside the coaxial structure. A conceptual scheme of the mechanism is depicted in Figure 2.

The coaxial nanoapertures were designed to be a single mode system, i.e., possessing a single allowed excitation for $l_{GM} = \pm 1$ (the analysis of the guided mode is presented in the Supporting Information). The spiral corrugation couples the incident light into a plasmonic wave and induces a dynamic spiral phase according to the spiral grating pitch, l_S . In this experiment (see Figure 1b) the corrugation structure adds a spiral phase with $l_S = 2$. We verified that *only* $l_S = 2$ provides spin-dependent transmission enhancement through the apertures. The exceptional transmission enhancement observed in the experiment indicates that the eigenmode of the coaxial waveguide was properly excited by a surface mode. The apparent difference between $l_{GM} = \pm 1$ and the spiral charge $l_S = 2$ of the surface mode leads one to assume that another mechanism induced an additional spin-dependent spiral phase that compensated for the excess of AM on the left side of the selection rule in eq 1. This phase modifies the complete OAM of the surface mode to be $l_{SM} = \sigma_{in} + l_S$ (σ_{in} is the incident spin), which now perfectly satisfies the AM selection rule of the system. Thus, the incident spin is converted into the OAM, conserving the total AM of the system. This photon spin–orbit coupling through surface plasmon excitation originates from a geometric Berry phase arising in the system.^{18–21}

The above effect can be regarded as a spatial angular Doppler effect (ADE).²² In analogy with a *temporal* ADE, where an observer at a reference frame rotating with a rate Ω_t registers a spin-dependent temporal frequency shift,²³ here a rotation of the periodic surface corrugation in space with Ω_ξ induces a spin-dependent *spatial* frequency shift. Accordingly, the geometric phase arising from this spatial frequency modulation can be easily calculated to be $\phi_g = -\sigma_{in}/\Omega_\xi d\xi$, where the grating rotates along the coordinate ξ by $\Omega_\xi = d\theta/d\xi$, where the angle θ indicates the local groove’s orientation. In the structure presented in Figure 1b where $\xi = \varphi$, the geometric phase is simply given by the spin-dependent spiral phase $\phi_g = -\sigma_{in}\varphi$ producing the required additional OAM for the surface wave to satisfy the

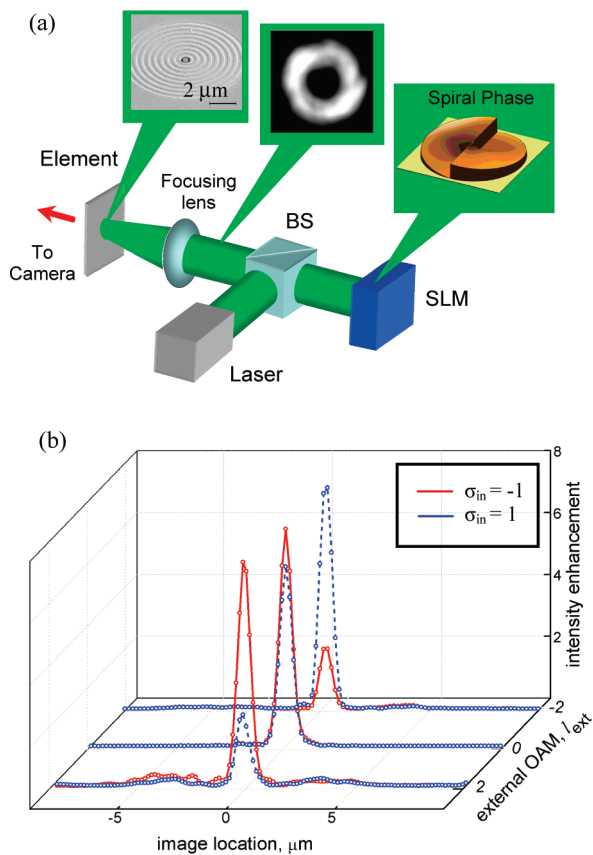


Figure 3. The removal of the spin-degeneracy in circular corrugation by use of externally induced OAM. (a) Experimental setup. A laser beam is modulated by a spatial light modulator (SLM) to obtain a spiral phase and then incident through a beam splitter (BS) onto a coaxial aperture with circular corrugation. The transmitted light is captured in the image plane by the camera. The spiral phase with $l_{\text{ext}} = 2$, the measured intensity distribution across the incident beam, and the SEM picture of the element are presented in the figure. (b) Intensity distribution cross sections captured by the camera for different l_{ext} . The blue dashed lines correspond to $|\sigma_+\rangle$ illumination and red solid lines correspond to $|\sigma_-\rangle$ illumination. The intensity was normalized by the transmission measured via a coaxial aperture without the surrounding corrugation (the horizontal dimension was scaled according to the optical magnification).

AM selection rule (eq 1). Note that while polarization and chirality effects in anisotropic inhomogeneous nanoscale structures were investigated previously,^{24–27} the mechanism of spin–orbit interaction was not distinguished.

In the second experiment the spin–orbit interaction mechanism and the AM selection rules were experimentally verified by investigating the effect in a circularly symmetric—*achiral*—nanostructure.

For this purpose we induced an external OAM carried by the incident beam instead of adding the OAM through a spiral surface corrugation. We fabricated the element on the same substrate, which consisted of an individual coaxial aperture with the same dimensions as before, surrounded by an annular coupling grating (see Figure 3a). This aperture was illuminated by a green laser light (Verdi of Coherent; $\lambda = 532$ nm) whose phase was modulated by a spatial light modulator (SLM Hamamatsu - PPM X8267) to achieve a spiral phase with $l_{\text{ext}} = 0, \pm 2$. The circular symmetry of

the coupling corrugation does not induce a dynamic phase, which means that $l_s = 0$. However, due to the spin–orbit interaction, the incident spin induces a spiral Berry phase and, as before, is converted to the OAM component of the surface mode. The external spiral phase modifies the complete OAM of the surface mode to be $l_{\text{SM}} = \sigma_{\text{in}} + l_{\text{ext}}$. Therefore, when the external OAM is zero, the resulting surface mode AM is $l_{\text{SM}} = \pm 1$, in which case the selection rule is *always* satisfied and the transmission of the element is undistinguished for distinct spin states. Moreover, providing an external spiral phase of $l_{\text{ext}} = 2$, the AM of the surface mode will be either 1 or 3 for an incident spin $|\sigma_-\rangle$ or $|\sigma_+\rangle$, respectively. For $l_{\text{ext}} = -2$, the surface mode AM will be correspondingly, -3 for $|\sigma_-\rangle$ and -1 for $|\sigma_+\rangle$. As before, the best overlapping of the surface mode and the guided mode is obtained for $l_{\text{SM}} = \pm 1$; therefore, the transmitted intensity will be strongly dependent upon the incident spin. Figure 3b shows the measured transmissions for various combinations of l_{ext} and σ_{in} . The transmission ratio of the two spin states was shown to be approximately 3 which is close to the ratio measured with the spiral corrugations. Thus, the suggested AM selection rule is verified for systems of substantially different symmetry.

Additional understanding of the AM evolution in the enhanced resonant transmission can be obtained by analyzing the AM of the light scattered from the nanoaperture. To do this, we investigated the scattered light far behind the element. The transverse electric field component of the guided mode²⁸ with $l_{\text{GM}} = 1$, can be described by the Jones vector

$$\mathbf{E}_r^{\text{GM}} = (E_x, E_y)^T = E_0(r)(\cos \varphi, \sin \varphi)^T e^{-i\varphi}$$

where $E_0(r)$ is the radial field dependence. Note that the guided mode in a circular basis is given by

$$\mathbf{E}_r^{\text{GM}} = E_0(r)[(1/\sqrt{2})|\sigma_+\rangle + (1/\sqrt{2})e^{-i2\varphi}|\sigma_-\rangle]$$

This field distribution corresponds to a vectorial vortex (see Figure 4a) with a *Pancharatnam* topological charge of 1, resulting in a total AM of $j = 1$. As was shown previously,²⁹ such vectorial vortices are unstable and collapse upon propagation. We have calculated the guided mode using finite difference time domain algorithm (FDTD) and propagated it to the far-field. The calculated far-field distribution was compared to the experimental measurement (see Figure 4 b–e).

As expected from the far-field of E_r^{GM} , we observed a bright and a dark spot for the left and right circular polarization components, respectively, with a good agreement between calculation and measurement. Thus, the total AM of light in our system is conserved also for the scattered light ($j = 1$). The analysis of the AM of the scattered light enables characterizing the allowed excitations in nanoscale systems.

In summary, we presented the effect of spin symmetry breaking via spin–orbit interaction, which occurs even in rotationally symmetric (*achiral*) structures. We explored a simple plasmonic nanostructure that can be resonantly excited only if an AM selection rule is fulfilled. This selection rule represents a matching of the angular momentum of the incident radiation with the excited plasmonic modes in the

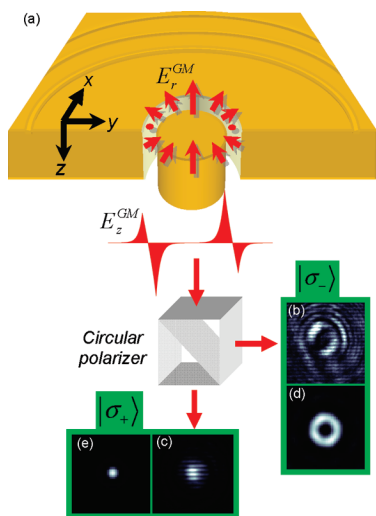


Figure 4. Far-field analysis of the light scattered from the element. (a) The E_z component distribution of the guided mode and the instantaneous transverse vectorial field (E_r). (b, c) Measured and (d, e) calculated intensity distributions of the light scattered to the far-field, for light transmitted through left-handed (b, d) and right-handed (c, e) circular polarizer.

system. During the excitation of the surface waves in a nanostructure, the incident spin AM is converted into the orbital AM of the surface plasmons, providing the OAM of the plasmonic mode, which is required for resonant light transmission through the nanoaperture. We believe that the suggested approach provides an additional physical insight by emphasizing the significant role of the spin-orbit interaction in the phenomenon of extraordinary light transmission, which until now has not been fully explained. The understanding of the AM selection rules in nanoscale structures can be exploited to investigate the excitation of a single molecule imbedded in plasmonic nanosystems.³⁰ The presented results provide a scientific and technological basis for more complex spin-based nanophotonic applications.

Supporting Information Available: Detailed discussion of the guided and the surface modes in the nanostructure. This material is available free of charge via the Internet at <http://pubs.acs.org>.

References

- (1) Bozhevolnyi, S. I.; Volkov, V. S.; Devaux, E.; Laluet, J.-Y.; Ebbesen, T. W. *Nature* **2006**, *440*, 508.
- (2) Fang, N.; Lee, H.; Sun, C.; Zhang, X. *Science* **2005**, *308*, 534.
- (3) Stockman, M. I. *Phys. Rev. Lett.* **2004**, *93*, 137404.
- (4) Lezec, H. J.; Degiron, A.; Devaux, E.; Linke, R. A.; Martin-Moreno, L.; Garcia-Vidal, F. J.; Ebbesen, T. W. *Science* **2002**, *297*, 820.
- (5) Pendry, J. B.; Martin-Moreno, L.; Garcia-Vidal, F. J. *Science* **2004**, *305*, 847.
- (6) Ebbesen, T. W.; Lezec, H. J.; Ghaemi, H. F.; Thio, T.; Wolff, P. A. *Nature* **1998**, *391*, 667.
- (7) Bryan-Brown, G. P.; Sambles, J. R.; Hutley, M. C. *J. Mod. Opt.* **1990**, *37*, 1227.
- (8) Cao, Q.; Lalanne, P. *Phys. Rev. Lett.* **2002**, *88*, 057403.
- (9) Yang, C. N. *Phys. Rev.* **1950**, *77*, 242.
- (10) Balling, L. C.; Wright, J. J. *Appl. Phys. Lett.* **1976**, *29*, 411.
- (11) Van Enk, S. J.; Nienhuis, G. *J. Mod. Opt.* **1994**, *41*, 963.
- (12) Poynting, J. H. *Proc. R. Soc. London, Ser. A* **1909**, *82*, 560.
- (13) Beth, R. A. *Phys. Rev.* **1936**, *50*, 115.
- (14) Van Enk, S. J.; Nienhuis, G. *Opt. Commun.* **1992**, *94*, 147.
- (15) O'Neil, A. T.; MacVicar, I.; Allen, L.; Padgett, M. J. *Phys. Rev. Lett.* **2002**, *88*, 053601.
- (16) Berry, M. V. *Proc. R. Soc. London, Ser. A* **1984**, *392*, 45.
- (17) Allen, L.; Beijersbergen, M. W.; Spreeuw, R. J. C.; Woerdman, J. P. *Phys. Rev. A* **1992**, *45*, 8185.
- (18) Gorodetski, Y.; Niv, A.; Kleiner, V.; Hasman, E. *Phys. Rev. Lett.* **2008**, *101*, 043903.
- (19) Liberman, V. S.; Zel'dovich, B. Ya. *Phys. Rev. A* **1992**, *46*, 5199.
- (20) Bliokh, K. Y.; Niv, A.; Kleiner, V.; Hasman, E. *Nat. Photonics* **2008**, *2*, 748.
- (21) Niv, A.; Gorodetski, Y.; Kleiner, V.; Hasman, E. *Opt. Lett.* **2008**, *33*, 2910.
- (22) Bliokh, K. Y.; Gorodetski, Y.; Kleiner, V.; Hasman, E. *Phys. Rev. Lett.* **2008**, *101*, 030404.
- (23) Garetz, B. A. *J. Opt. Soc. Am.* **1981**, *71*, 609.
- (24) Schwanecke, A. S.; Fedotov, V. A.; Khardikov, V. V.; Prosvirmin, S. L.; Chen, Y.; Zheludev, N. I. *Nano Lett.* **2008**, *8*, 2940.
- (25) Kuwata-Gonokami, M.; Saito, N.; Ino, Y.; Kauranen, M.; Jefimovs, K.; Vallius, T.; Turunen, J.; Svirko, Y. *Phys. Rev. Lett.* **2005**, *95*, 227401.
- (26) Drezet, A.; Genet, C.; Laluet, J.-Y.; Ebbesen, T. W. *Opt. Express* **2008**, *16*, 12559.
- (27) Ohno, T.; Miyanishi, S. *Opt. Express* **2006**, *14*, 6285.
- (28) Lockyear, M. J.; Hibbins, A. P.; Sambles, J. R.; Lawrence, C. R. *Phys. Rev. Lett.* **2005**, *94*, 193902.
- (29) Niv, A.; Biener, G.; Kleiner, V.; Hasman, E. *Opt. Express* **2006**, *14*, 4208.
- (30) Rigneault, H.; Capoulade, J.; Dintinger, J.; Wenger, J.; Bonod, N.; Popov, E.; Ebbesen, T. W.; Lenne, P.-F. *Phys. Rev. Lett.* **2005**, *95*, 117401.

NL901437D